P 1.1 Effective Bulk Shear in Supercell Thunderstorm Environments

Richard L. Thompson*, Corey M. Mead, and Roger Edwards
Storm Prediction Center
Norman, OK

1. Introduction

Supercell[a] thunderstorm environments, both from observations and numerical simulations, typically are characterized by relatively large buoyancy and vertical shear through a substantial depth of the troposphere. Based largely on the numerical simulations of Weisman and Klemp (1982; 1984), the depth of the vertical shear layer relevant to supercell formation has been defined as the lowest 4-6 km above ground level (AGL). While measures of vertical shear such as 0-6 km bulk shear and the bulk Richardson number shear term have proven successful in identifying supercell potential from environmental soundings (e.g., Rasmussen and Blanchard 1998; Thompson et al. 2003, hereafter T03), each of these shear parameters represents an arbitrary fixed layer. Such fixed layer parameters become less reliable when attempting to characterize environments of very tall storms (e.g., high equilibrium level (EL) heights), very short storms, or storms not rooted near the surface (so-called "elevated" thunderstorms). As an alternative to fixed layer shear depths, vertical shear can be defined with respect to a measure of the depth a particular storm (i.e., the lifted parcel height to EL height). In this way, vertical shear measures can be normalized such that very tall storms, relatively shallow storms, and elevated storms can be compared in a consistent and potentially meaningful way.

* *Corresponding author address:* Richard L. Thompson, 1313 Halley Circle, Norman, OK 73069. Email: Richard.thompson@noaa.gov

2. Data and Methodology

The RUC model close proximity sounding sample described in T03 has been augmented to include additional storm cases from 2003 and 2004, increasing the entire sample size to 916 soundings - the same sounding sample used by Thompson et al. (2004a) in the companion paper describing effective storm-relative helicity. Details regarding the sounding collection methodology can be found in Edwards et al. (2004). The most unstable lifted parcel height and the resultant EL height were calculated for each proximity sounding, and these heights were used as lower and upper bounds to the storm depth, respectively. Bulk vertical shear was then calculated for ten equally deep layers within the storm, and the bulk shear through these layers is referred to as the effective bulk shear.

An illustration of the the effective shear technique is provided in Fig. 1. The sounding displayed in Fig. 1 was associated with a right-moving supercell in an environment with no surface-based CAPE (after Doswell and Rasmussen 1994), but a most-unstable parcel CAPE of 1350 J kg^{-1}. The most unstable parcel level (825 hPa in the sounding in Fig. 1, or 1436 m AGL) marks the "base" of the storm layer, while the equilibrium level (~205 hPa on the sounding in Fig. 1, or 11,736 m AGL) marks the "top" of the storm layer. Translating this effective storm layer to a hodograph, the effective vector shear for the lower half of the storm depth (as discussed in Section 3) is shown in Fig. 2. Note that the effective

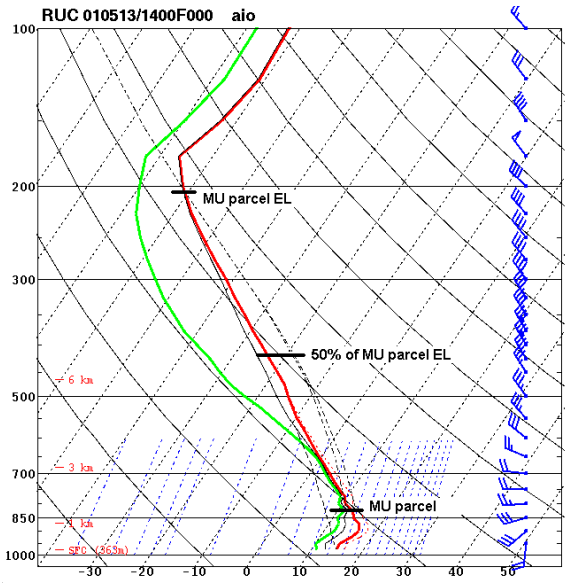

Figure 1. Skew-t log P plot of a RUC model proximity sounding for an elevated right-moving supercell from 13 May 2001 at 1400 UTC. Marked by heavy horizontal lines on the sounding plot are the heights of the most unstable (MU) parcel, the MU parcel equilibrium level (EL) height, and 50% of the depth from the MU parcel height to the EL height.

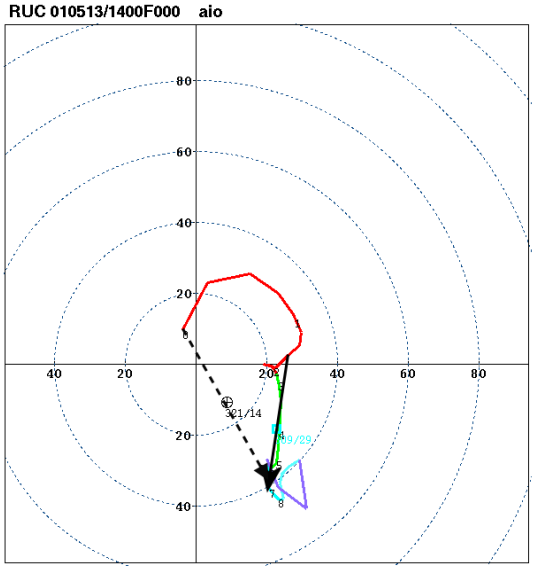

Figure 2. Hodograph plot of the wind profile (kt) associated with the sounding shown in Fig. 1. The color coded bands denote every 3 km from the ground to 12 km AGL, beginning with red for the lowest 3 km. The hodograph is annotated with the effective shear vector (solid black) through the lowest half of the storm depth (50% of MU parcel EL marked in Fig. 1), and the 0-6 km shear vector (dashed black).

vector shear magnitude is a little smaller than the standard 0-6 km vector shear, while the orientation of the effective shear vector is from the north-northeast to the south-southwest, as opposed to a northwest to southeast orientation for the 0-6 km shear.

3. Results

From the sample of 916 RUC model supercell proximity soundings, it is seen that effective bulk shear tends to increase through the depth of the storm for both supercells and nonsupercells, though the effective shear is usually much stronger for the supercells (Fig. 3). Not surprisingly, the

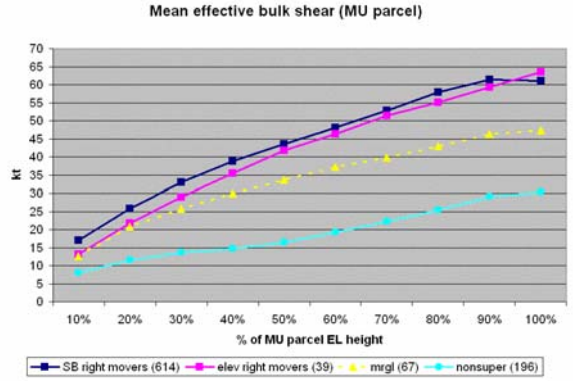

Figure 3. Plot of mean effective bulk shear (kt) for ten equal layers from the height of the MU parcel upward to the EL. Values on the abscissa denote the % of MU parcel to EL depth, where "10%" represents the MU parcel upward to 10% of the EL height, etc. Four storm groups are shown: surface-based supercells (SB right movers), elevated right-moving supercells (elev right movers), surface-based storms with marginal supercell characteristics (mrgl), and discrete, surface-based nonsupercells (nonsuper). Sounding sample sizes are given in parentheses.

effective shear associated with storms displaying "marginal" supercell characteristics (see T03) tended to fall between the supercells and discrete nonsupercell storms. An alternative view of the effective shear is shown in Fig. 4 in the form of a line plot derived from percentile rank distributions for the different storm groups. In Fig. 4, the plot of the 10th

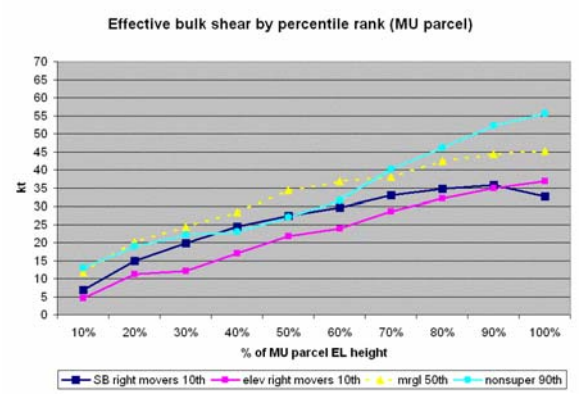

Figure 4. Selected percentile rank plots of effective bulk shear by percentage of storm depth. The lines plotted are: 10th percentile for surface-based supercells (dark blue), 10th percentile for elevated right-moving supercells, the median values for marginal supercells, and the 90th percentile for nonsupercells. Other figure conventions are the same as Fig.3.

percentile effective shears with the supercells is compared to the 90th percentile effective shears with the nonsupercells. The difference in the y axis is equivalent to the degree of overlap between 1) the bottom of a box and whiskers distribution for the supercells, and 2) the top whisker with the nonsupercells. The overlap in the effective shear distributions between supercells and nonsupercells is largest in the upper and lower portions of the storms, as evidenced by the larger effective shear values for the nonsupercells in the lower 20% and upper 30% of normalized storm depth. However, the 90th percentile effective shears with the nonsupercells are roughly the same as the 10th percentile values for the surface-based supercells in the range of 40-60% of the storm depths. This suggests that the difference between supercells and nonsupercells is most pronounced in the middle portions of the storms, and hereafter we refer to the effective shear through the lower half of each storm as the "effective shear".

The effective shear corresponds to 0-6 km AGL for most surface-based storms in our sample with EL heights ranging from 11-13 km AGL. The effective shear magnitude discriminates strongly between supercell and nonsupercell storms (Fig. 5), similar to the 0-6 km bulk shear. The differences in the fixed layer and effective layer approaches becomes more apparent when comparing surface-based supercell and elevated supercell soundings. As shown in Fig. 6, the 0-6 km bulk shear is substantially stronger for the elevated supercells than for the surface-based, nontornadic supercells. However, the effective shear is very similar for each storm group. The fixed layer shear includes the near-ground layer, which often contains large vertical shear in elevated supercell environments such as poleward of a surface warm front (refer to Figs. 1 and 2). By starting the effective shear calculation at the most unstable parcel height, the effective shear avoids inclusion of large near-ground shear that may not be associated with any buoyancy. Therefore, the effective shear appears to provide a more reasonable estimation of the vertical shear relevant to elevated supercells, while replicating the

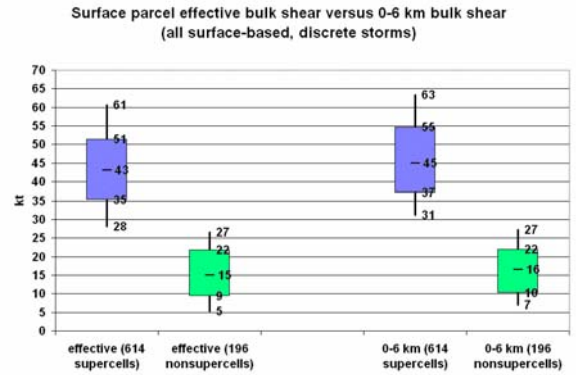

Figure 5. Box and whiskers plot of effective bulk shear (through the lowest half of the storm depth) and the fixed layer 0-6 km bulk shear for surface-based supercells and discrete, surface-based nonsupercells. The shaded boxes enclose the 25th percentile (bottom of box) to the 75th percentile values, with the median value denoted within the box. The whiskers extend upward to the 90th percentiles, and downward to the 10th percentiles. Sounding sample sizes are given in parentheses.

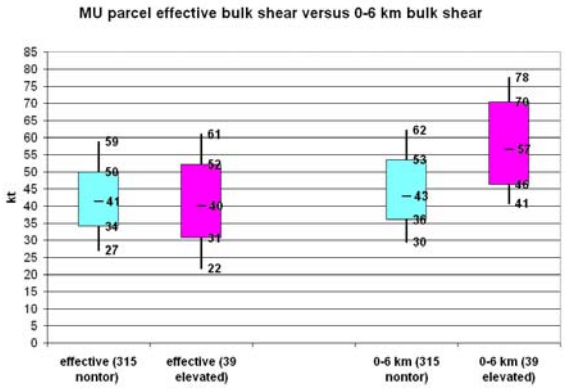

Figure 6. Box and whiskers plot of effective bulk shear and 0-6 km bulk shear for 315 proximity soundings associated with nontornadic, surface-based supercells, and 39 proximity soundings associated with elevated, right-moving supercells. Other conventions are the same as Fig. 5.

ability of the 0-6 km bulk shear to discriminate between surface-based supercells and nonsupercells.

Another concern with fixed layer shear calculations is when a storm is particularly tall or short. For example, the 0-6 km bulk shear represents only the bottom 35-40% of the highest EL case storm depths in our supercell sample, but it extends through 75-90% of the storm depth in our lowest EL cases. The 0-6 km bulk shear and effective shear comparison in Fig. 5 shows little difference between the two techniques because that sample is dominated by storms with EL heights in a relatively narrow range from 11 to 13 km above ground level. However, the results differ when considering only the tallest storms (highest 10% of EL heights) and the shortest storms (lowest 10% of EL heights). As shown in Fig. 7, the effective shear approach has a large impact on the bulk shear values associated with the shortest storms. The effective shear values are substantially smaller with the shortest supercells (61 cases with EL heights < ~8500 m AGL), and slightly greater with the tallest storms (61 cases with EL heights > ~13,500 m AGL).

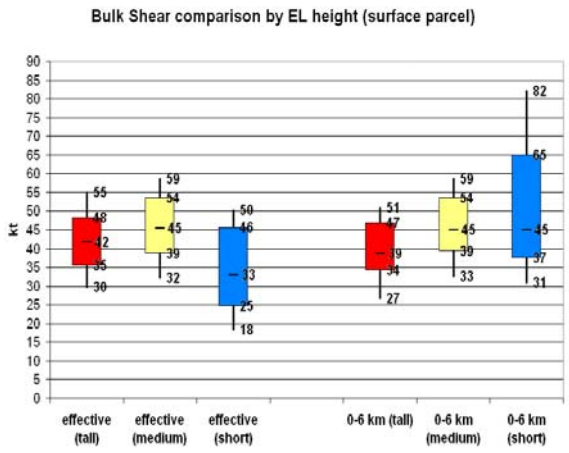

Figure 7. Box and whiskers plot of effective bulk shear and 0-6 km bulk shear for three equal size groups (61 soundings) of surface-based, right-moving supercells. The "tall" storms represent the highest 10% of EL heights, the "medium" storms are 5% either side of the median EL height, and the "short" storms are the lowest 10% of EL heights. Other conventions are the same as Fig. 5.

An explanation for the larger impact on the shortest storms, as compared to the tallest storms, is that the shortest storms have EL heights 40-65% of the median EL height in our sample (11,697 m AGL), while the tallest storms have EL heights only 10-30% higher than the median storm.

When viewed through a large depth, other differences become apparent between the effective shear and the fixed layer shear. First, mean bulk shear is largest through the lowest 10 km AGL for the shortest supercells, with the greatest differences near 10 km AGL (Fig. 8). Second, the fixed layer mean bulk shear is smallest for the tallest storms, though values are closer to the "medium" supercells above 5 km AGL. The pattern is reversed in the low-middle parts of the storms when considering effective shear (Fig. 9). The shortest storms were associated with the weakest shear, while the tallest storms and the typical storms were quite similar in the lowest 80% of normalized storm depth.

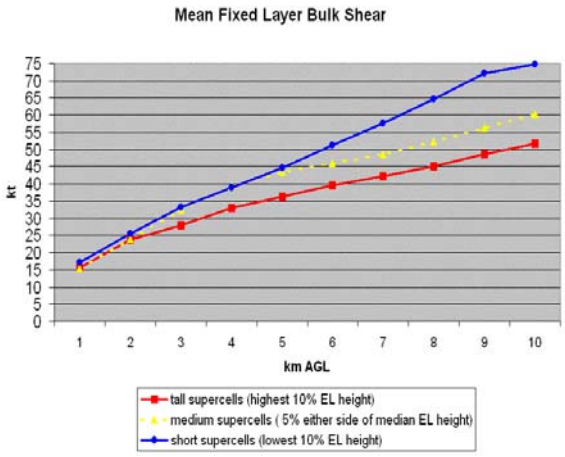

Figure 8. Plot of mean fixed layer bulk shear from the ground upward to 10 km AGL for the same "tall", "medium", and "short" supercell groups in Fig. 7.

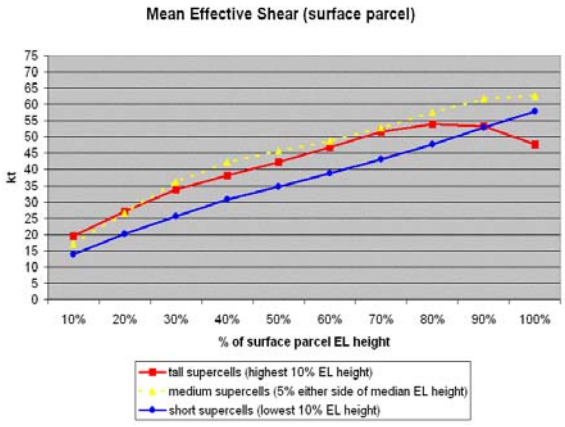

Figure 9. Plot of mean effective bulk shear by percentage of storm depth for the same "tall", "medium", and "short" supercell groups in Fig. 7.

4. Conclusions

The effective shear, much like the fixed layer 0-6 km AGL shear, discriminates strongly between supercell and nonsupercell thunderstorms. The effective shear normalizes the shear values for shallow and very tall storms, allowing more realistic assessments of these storm profiles. Effective shear was weakest near the top of the tallest storms - possibly due to the tendency for the tallest storms to occur later in the warm season when tropospheric flow is usually weaker than during the cool season. The use of the most unstable parcel height in the effective shear calculation also allows elevated supercell environments to be treated similarly to surface-based storm environments, and the effective shear approach identifies the relevant shear impacting elevated storms. Given its flexibility to represent both surface-based and elevated supercell environments, the effective shear should be used as a replacement for the fixed 0-6 km shear in composite indices such as the supercell composite parameter (Thompson et al. 2004b).

Finally, though EL heights with the supercells in our multi-year sample did not exceed 15,800 m, there is still the possibility for the supercell potential of environments associated with very high-topped storms (such as 28 August 1990 Plainfield, IL (Korotky et al. 1993) and 27 May 1997 Jarrell, TX (see Corfidi 1998)) to be under-estimated with the fixed layer approach.

5. Acknowledgments

We thank Steve Weiss for his thought provoking review of this manuscript, and John Hart for providing programming assistance with the early versions of our calculations.

6. References

Edwards, R., R. L. Thompson, and C. M. Mead, 2004: Assessment of anticyclonic supercell environments using close proximity soundings from the RUC model. Preprints, *22nd Conf. on Severe Local Storms*, Hyannis, MA, Amer. Meteor. Soc., (this volume).

Corfidi, S. F., 1998: Some thoughts on the

role mesoscale features played in the 27 May 1997 central Texas tornado outbreak. Preprints, *19th Conf. on Severe Local Storms*, Minneapolis, MN, Amer. Meteor. Soc, 177-180.

Doswell, C. A. III, and E. N. Rasmussen, 1994: The effect of neglecting the virtual temperature correction on CAPE calculations. *Wea. Forecasting*, **9**, 625-629.

Korotky, W., R. W. Pryzbylinski, and J. A. Hart, 1993: The Plainfield, Illinois, tornado of August 28, 1990: The evolution of synoptic and mesoscale environments. *The Tornado: Its Structure, Dynamics, Prediction, and Hazards, Geophys. Monogr*., No. 79, Amer. Geophys. Union, 611-624.

Rasmussen, E. N., and D. O. Blanchard, 1998: A baseline climatology of sounding-derived supercell and tornado parameters. *Wea. Forecasting*, **13**, 1148-1164.

Thompson, R. L., C. M. Mead, and R. Edwards, 2004a: Effective storm-relative helicity in supercell thunderstorm environments. Preprints, *22nd Conf. on Severe Local Storms*, Hyannis, MA, Amer. Meteor. Soc., (this volume).

_____, R. Edwards, and C. M. Mead, 2004b: An update to the supercell composite and significant tornado parameters. Preprints, *22nd Conf. on Severe Local Storms*, Hyannis, MA, Amer. Meteor. Soc., (this volume).

_____, R. Edwards, J. A. Hart, K. L. Elmore, and P. M. Markowski, 2003: Close proximity soundings within supercell environments obtained from the Rapid Update Cycle. *Wea. Forecasting*, **18**, 1243-1261.

Weisman, M. L., and J. B. Klemp, 1982: The dependence of numerically simulated convective storms on vertical wind shear and buoyancy. *Mon. Wea. Rev*., **110**, 504-520.

_____, _____, 1984: The structure and classification of numerically simulated convective storms in directionally varying wind shears. *Mon. Wea. Rev*., **112**, 2479-2498.